This is an open access article published under an ACS AuthorChoice License, which permits copying and redistribution of the article or any adaptations for non-commercial purposes.

JACS
JOURNAL OF THE AMERICAN CHEMICAL SOCIETY
Article
pubs.acs.org/JACS

ω-Alkynyl Lipid Surrogates for Polyunsaturated Fatty Acids: Free Radical and Enzymatic Oxidations

William N. Beavers,[†,∥] Remigiusz Serwa,[†,∥,⊥] Yuki Shimozu,[‡] Keri A. Tallman,[†] Melissa Vaught,[†] Esha D. Dalvie,[§,#] Lawrence J. Marnett,[†,‡,§] and Ned A. Porter*[,†,‡]

A.B. Hancock Memorial Laboratory for Cancer Research, Departments of [†]Chemistry, [‡]Biochemistry, and [§]Pharmacology, Vanderbilt Institute for Chemical Biology, Vanderbilt Center in Molecular Toxicology, Vanderbilt Ingram Cancer Center, Vanderbilt University, Nashville, Tennessee 37235, United States

Supporting Information

ABSTRACT: Lipid and lipid metabolite profiling are important parameters in understanding the pathogenesis of many diseases. Alkynylated polyunsaturated fatty acids are potentially useful probes for tracking the fate of fatty acid metabolites. The nonenzymatic and enzymatic oxidations of ω-alkynyl linoleic acid and ω-alkynyl arachidonic acid were compared to that of linoleic and arachidonic acid. There was no detectable difference in the primary products of nonenzymatic oxidation, which comprised *cis*,*trans*-hydroxy fatty acids. Similar hydroxy fatty acid products were formed when ω-alkynyl linoleic acid and ω-alkynyl arachidonic acid were reacted with lipoxygenase enzymes that introduce oxygen at different positions in the carbon chains. The rates of oxidation of ω-alkynylated fatty acids were reduced compared to those of the natural fatty acids. Cyclooxygenase-1 and -2 did not oxidize alkynyl linoleic but efficiently oxidized alkynyl arachidonic acid. The products were identified as alkynyl 11-hydroxy-eicosatetraenoic acid, alkynyl 11-hydroxy-8,9-epoxy-eicosatrienoic acid, and alkynyl prostaglandins. This deviation from the metabolic profile of arachidonic acid may limit the utility of alkynyl arachidonic acid in the tracking of cyclooxygenase-based lipid oxidation. The formation of alkynyl 11-hydroxy-8,9-epoxy-eicosatrienoic acid compared to alkynyl prostaglandins suggests that the ω-alkyne group causes a conformational change in the fatty acid bound to the enzyme, which reduces the efficiency of cyclization of dioxalanyl intermediates to endoperoxide intermediates. Overall, ω-alkynyl linoleic acid and ω-alkynyl arachidonic acid appear to be metabolically competent surrogates for tracking the fate of polyunsaturated fatty acids when looking at models involving autoxidation and oxidation by lipoxygenases.

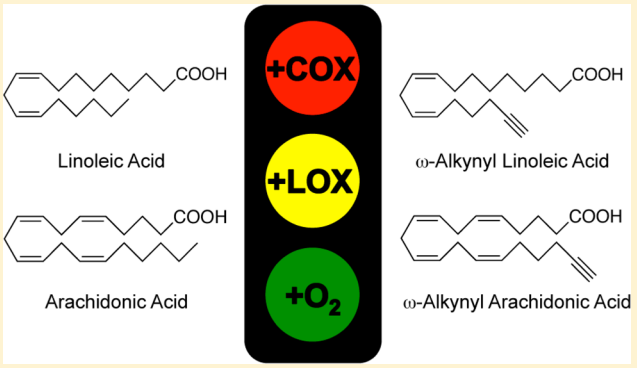

INTRODUCTION

The lipidome is a complex mixture of fatty acid and sterol molecular species, which include the fatty acid esters of sterols, triglycerides, and glycerophospholipids, such as the ethanolamines, cholines, and inositols.[2] Polyunsaturated fatty acids (PUFAs) such as linoleic acid (LA) (18:2) and arachidonic acid (AA) (20:4) and their esters are particularly important molecular species. These essential fatty acids are involved in a number of consequential metabolic transformations via their oxidation by lipoxygenase (LOX) and cyclooxygenase (COX) enzymes.[3−6] Oxidized lipids play a significant role in a number of physiological and pathophysiological events, including cardiovascular disease, cancer, and neurodegenerative diseases.[7] The nonenzymatic peroxidation of both LA and AA by molecular oxygen generates intermediate peroxyl free radicals.[8−12] Products that result from this lipid peroxidation include peroxides and hydroperoxides, as well as secondary electrophilic products capable of covalently modifying biomolecules, potentially altering their function.[13−16]

Tracking lipids, lipid metabolites, and lipid decomposition products in cells is a formidable task as the complexity of the mixture challenges the most powerful analytical tools.[17−20] Stable isotope derivatives of lipids have been used with some success to track the distribution of molecular species into different lipid classes in organelles, but detecting a minor metabolic byproduct from thousands of different lipid species is particularly difficult since stable isotope-labeled compounds are often isobaric with endogenous species.[21] Radiolabels have also been used successfully in many applications, but associating a particular radioactive chromatography fraction with the structure of a molecular species in a complex mixture is a challenge. Recently, an affinity labeling technique that makes use of terminal alkynyl lipid analogues was reported.[22] In this approach, stable, but reversible, alkyne−cobalt complexes are formed on a phosphine-modified silica to isolate alkynyl lipids. This strategy has been used to monitor the distribution of

Received: June 16, 2014
Published: July 17, 2014

 © 2014 American Chemical Society dx.doi.org/10.1021/ja506038v | J. Am. Chem. Soc. 2014, 136, 11529−11539

alkynyl fatty acids into various cellular phospholipid classes along with the subsequent lipase-catalyzed metabolism of those lipids.[23] In recent studies, terminal alkynyl analogues of 4-hydroxy-2*E*-nonenal (HNE) and 4-oxo-2*E*-nonenal (ONE), lipid-derived electrophiles known to modify proteins and nucleic acids, were used to globally profile electrophile adduction of proteins. UV-cleavable biotin azide was used to isolate, identify, and quantify cellular protein−electrophile adducts.[16,24,25] This affinity chemistry allows protein−lipid adducts to be concentrated and identified by standard proteomic protocols. One shortcoming of adding electrophiles exogenously to cells is that it does not mimic endogenous lipid electrophile diversity, concentration, time course of generation, and location of formation. To address these issues, we have developed a series of ω-alkynyl PUFAs to investigate endogenous lipid oxidation and its cellular consequences.

Tracking lipid incorporation and metabolism in cellular systems has long been a goal for chemists, biochemists, and biologists alike. Alkynyl analogues of lipid and cholesterol species have been utilized to facilitate the tracking and retrieval of these species in cells.[16,22,26] During these studies, it is assumed that the ω-alkyne confers only a minimal structural change to its lipid analogue, resulting in nearly identical chemical, biochemical, and biological properties. Here, we report the oxidation chemistry for the alkynyl lipid analogues, *a*AA and *a*LA, revealing that alkyne substitution has no effect on fatty acid free radical autoxidation, and minimal effect on enzymatic oxidation. This establishes that alkynyl PUFAs provide a method to selectively study lipid distribution, chemistry, and lipid metabolite interactions with cellular macromolecules.

EXPERIMENTAL SECTION

Materials. All reagents are from Sigma, St. Louis, MO, unless otherwise noted. All native fatty acids and deuterated lipid metabolites are from Cayman Chemical, Ann Arbor, MI, unless otherwise noted. The alkynyl fatty acids, *a*LA and *a*AA, were synthesized as previously described.[26] *N*-methyl benzohydroxamic acid (NMBHA) has been prepared as previously described.[27] Benzene (HPLC grade) was passed through a column of neutral alumina and stored over molecular sieves (benzene is a carcinogen and mutagen, and should be used with extreme care). Commercial α-tocopherol was chromatographed before use. Diazomethane was prepared by portion-wise addition of nitrosomethylurea into heterogeneous mixture of 40% aqueous KOH and ethanol at 0 °C. The deep-yellow organic layer was decanted and dried over NaOH. The dried ethereal MeN_2 was used immediately.

Formation and Analysis of Alkynyl Hydroxy Octadecadienoic Acid (*a*HODE) by Autoxidation. To a solution of *a*LA in benzene was added 2,2′-azobis(4-methoxy-2,4-dimethylvaleronitrile) (MeOAMVN) in benzene, and the mixture was incubated at 37 °C. After 45 min, a solution of butylated hydroxytoluene (BHT) and triphenyl phosphine (PPh_3) in benzene was added, and the mixture was vortexed for 1 min. Benzene was evaporated under a stream of argon, and the residual material was reconstituted in 1.2% isopropanol in hexanes with 0.1% acetic acid for HPLC-UV analysis. For direct infusion MS studies of *a*HODE, eluted peaks from HPLC-UV analysis were collected, and solvents were evaporated under a stream of argon; then the residues were reconstituted in methanol. For NMR studies of *a*HODE, corresponding peaks collected from HPLC-UV analysis were combined, solvents were evaporated, and the residues were dried under high vacuum for 2 h. These dried materials were reconstituted in benzene-d_6 and placed into 1.7 mm OD sample tubes for NMR analysis.

Formation and Analysis of Alkynyl Hydroxy Eicosatetraenoic Acid (*a*HETE) by Autoxidation. To a mixture of *a*AA and NMBHA in acetonitrile was added MeOAMVN in acetonitrile. After 35 h of incubation at 37 °C, BHT/PPh_3 in acetonitrile was added, and the mixture was vortexed for 2 min. Acetonitrile was removed under a stream of argon, and the remaining material was reconstituted in 1.2% isopropanol in hexanes with 0.1% acetic acid for HPLC-UV analysis. MS studies of *a*HETE and NMR studies of *a*HETE were performed as described above for *a*HODE.

HPLC−UV/MS analysis of (*a*)HODEs and (*a*)HETEs. All HPLC Analyses of (*a*)HETE and (*a*)HODE were carried out on a single Beckman 5 μm ultrasphere silica column (250 mm × 4.6 mm) using isocratic normal phase conditions (1.2% IPA in hexanes containing 0.1% acetic acid).[28] Chiral HPLC analyses of HETE and HODE methyl esters were performed on a Chiralpak AD column (250 mm × 4.6 mm) produced by Chiral Technologies Inc., Exton, PA. *a*HETE products have been eluted with 2% ethanol in hexanes, whereas *a*HODE were eluted with 5% methanol in hexanes. Direct infusion MS experiments were performed on ThermoFinnigan TSQ Quantum triple quadrupole mass spectrometer, whereas all HPLC/MS analyses were conducted on the same instrument coupled with a Surveyor MS Pump and Surveyor Autosampler (for RP-HPLC) or with Waters Alliance 2690 Separation Module (NP-HPLC). Detailed information about solvent gradients and MS settings applied during these analyses is given in the appropriate protocols presented below. Unless stated otherwise, all the HPLC separations were conducted with a solvent flow rate of 1 mL/min.

Formation and Analysis of Alkynyl $F_{2\alpha}$-Isoprostane (*a*$F_{2\alpha}$-IsoP). MeOAMVN was added to a 165 mM solution of aAA in benzene, and the mixture was incubated at 37 °C for 24 h. Solvent was then evaporated, and the residue was treated with mixture of 1 mmol BHT and 10 mmol $P(OMe)_3$ in 3:1, acetonitrile/water and vortexed for 5 min. The following solvent gradient was applied: 10% (95:5, acetonitrile/methanol) in 2 mM ammonium acetate was held for 10 min, then ramped to 25% (95:5, acetonitrile/methanol) in 2 mM ammonium acetate over 45 min. LC/MS/MS with negative ion mode electrospray ionization (ESI) was used, and the important mass spectrometer parameters were optimized for commercially available $PGF_{2\alpha}$. The *m*/*z* transitions monitored were for *a*5$F_{2\alpha}$-IsoP (349 > 115), *a*8$F_{2\alpha}$-IsoP (349 > 127), *a*12$F_{2\alpha}$-IsoP (349 > 151), and *a*15$F_{2\alpha}$-IsoP (349 > 193). Control oxidations of AA were performed using analogous reaction conditions; however, slightly different analytical conditions were applied to analyze the AA oxidation products. The following solvent gradient was applied for AA oxidation products: 20% (95:5, acetonitrile/methanol) in 2 mM ammonium acetate was held for 10 min, then ramped to 40% (95:5, acetonitrile/methanol) in 2 mM ammonium acetate over 40 min. The *m*/*z* transitions monitored were for 5$F_{2\alpha}$-IsoP (353 > 115), 8$F_{2\alpha}$-IsoP (353 > 127), 12$F_{2\alpha}$-IsoP (353 > 151), and 15$F_{2\alpha}$-IsoP (353 > 193).

Cyclooxygenase O_2 Uptake Kinetics. Quantification of cyclooxygenase activity was performed in a thermostated cuvette at 37 °C with stirring and monitored using a polarographic electrode with an Instech System 203 oxygen monitor (Instech Laboratories Inc., Plymouth Meeting, PA). Substrates were solubilized in dimethyl sulfoxide (DMSO). Activity assays were performed in 100 mM Tris buffer containing 500 μM phenol, with hematin-reconstituted cyclooxygenase protein. Substrate concentration was varied (1−50 μM), and maximal reaction velocity data were obtained from the linear portion of the oxygen uptake curves. The data were analyzed by nonlinear regression with GraphPad Prism (GraphPad, San Diego, CA).

Crude Lipoxygenase Kinetic Parameters. LOX activity was detected by monitoring the absorbance of the conjugated diene product, HpETE, at 235 nm. UV assays were monitored using a Hewlett-Packard 8453 diode array spectrophotometer equipped with a thermostated cuvette at 25 °C, with stirring at 180 rpm. The enzyme reactions included reaction buffer 50 mM Tris pH 7.4 with 0.03% Tween-20 and substrate, and were initiated by the addition of enzyme. Compounds were dissolved in acetonitrile containing 10% acetic acid before addition to the reaction buffer; acetonitrile was kept below 1% of the total reaction volume. Substrate concentration was varied (1−50 μM), and maximal reaction velocity data were obtained from the linear

portion of the absorbance curves. Rates were converted from absorbance units/s to μM *a*HpETE/s using the molar absorptivity constant of 0.027 μM^{-1} cm^{-1}. The data were analyzed by nonlinear regression with GraphPad Prism.

Kinetic Measurements of *a*LA, LA, *a*AA, and AA by s15LOX1. s15LOX1, LA, AA, *a*LA, and *a*AA were all diluted to 2× final concentration in 100 mM borate pH 9 at 25 °C. One mL fatty acid was added to a 1 cm cuvette in a Beckman-Coulter DU-800 spectrophotometer as a blank control. One mL enzyme was added, and the reaction was monitored at 235 nm sampling every 1.5 s in triplicate. The slope was averaged over 10 points in the linear portion of the curve to get the Δabsorbance per second, which was converted to V_o using the molar extinction coefficients of 0.023 μM^{-1} cm^{-1} for HpODE and 0.027 μM^{-1} cm^{-1} for HpETE. Kinetic parameters were determined in GraphPad Prism using Michaelis−Menten fitting.

Enzymatic Oxidation of *a*LA and LA for LC/MS/MS Analysis. Soybean 15 lipoxygenase 1 (s15LOX1) (Cayman Chemical) was diluted to have a final concentration ratio of 100:1, fatty acid/enzyme in 100 mM borate pH 9. Potato 5 lipoxygenase (5LOX) (Cayman Chemical) was diluted to have a final concentration ratio of 100:1, fatty acid/enzyme, in 100 mM phosphate pH 6.3. LA and *a*LA were added from 100× stocks in DMSO, and incubated 15 min at 25 °C. The reactions were quenched and fatty acid metabolites extracted with ethyl acetate containing 0.5% acetic acid, PPh_3, ± 9-HODE-d_4, and ±13-HODE-d_4. Organic layer was dried under inert gas and dissolved in methanol for LC/MS/MS analysis. Metabolites were analyzed on a Thermo Finnigan TSQ Quantum with ESI source interfaced to Surveyor MS Pumps and Surveyor Autosampler in both full scan and SRM modes. Metabolites were separated by reverse-phase gradient HPLC on a C_{18} (50 mm × 2.1 mm, 3 μm) column (Supelco, St. Louis, MO) using 0.1% formic acid in water and 0.1% formic acid in acetonitrile as the A and B mobile phases, respectively. Full scan samples were separated by holding 20% B for 2 min, then ramping to 98% B over 6 min, holding 98% B for 3 min, then equilibrating to 20% B for 3 min. Q1 was scanned in negative ion mode from 250 m/z to 380 m/z in 1 s. SRM samples were separated by holding 40% B for 0.5 min, then ramping to 98% B over 2 min, holding at 98% B for 2 min, then equilibrating to 40% B for 2.5 min. Metabolites were detected by SRM in negative ion mode observing the m/z transitions for *a*9-HODE (291.2 > 171.2), *a*13-HODE (291.2 > 195.2), 9-HODE (295.2 > 171.2), 13-HODE (295.2 > 195.2), 9-HODE-d_4 (299.2 > 172.2), and 13-HODE-d_4 (299.2 > 198.2) for 100 ms each.

Mouse COX2 (mCOX2) was diluted to have a final concentration ratio of 100:1, fatty acid/enzyme in 100 mM Tris, 500 μM phenol, 2× [mCOX2] hematin pH 8. The mCOX2 was incubated 5 min at 37 °C. LA and *a*LA were added from 100× stocks in DMSO, and incubated 15 min at 37 °C. The reactions were quenched and fatty acid metabolites extracted and analyzed as detailed for the lipoxygenase enzymes.

Enzymatic Oxidation of *a*AA and AA for LC/MS/MS Analysis. s15LOX1 was diluted to a final concentration ratio of 100:1, fatty acid/enzyme, in 100 mM borate pH 9. AA and *a*AA were diluted to 100× stocks in DMSO. Fatty acids were separately added to enzyme solutions, and incubated 15 min at 25 °C. The reactions were quenched and fatty acid metabolites extracted with ethyl acetate containing 0.5% acetic acid, PPh_3, and ±15-HETE-d_8. The organic layer was dried under inert gas and dissolved in methanol for LC/MS/MS analysis. Metabolites were analyzed on a Thermo Finnigan TSQ Quantum with ESI source interfaced to Surveyor MS Pumps and Surveyor Autosampler in both full scan and SRM modes. Metabolites were separated by gradient HPLC on a C_{18} (50 mm × 2.1 mm, 3 μm) column using 0.1% formic acid in water and 0.1% formic acid in acetonitrile as the A and B mobile phases, respectively. Full scan samples were separated by holding 20% B for 2 min, then ramping to 98% B over 6 min, holding 98% B for 3 min, then equilibrating to 20% B for 3 min. Q1 was scanned in negative ion mode from 250 m/z to 380 m/z in 1 s. SRM samples were separated by holding 40% B for 0.5 min, then ramping to 98% B over 2 min, holding at 98% B for 2 min, then equilibrating to 40% B for 2.5 min. Metabolites were detected by SRM in negative ion mode observing the m/z transitions for *a*15-HETE (315.2 > 253.2), 15-HETE (319.2 > 257.2), and 15-HETE-d_8 (327.2 > 264.2) for 100 ms each.

mCOX2 was diluted to a final concentration ratio of 100:1, fatty acid/enzyme in 100 mM Tris, 500 μM phenol, 2× [mCOX2] Hematin pH 8. The mCOX2 was incubated 5 min at 37 °C. AA and *a*AA were added from 100× stocks in DMSO, and incubated 15 min at 37 °C. The reactions were quenched and fatty acid metabolites extracted and analyzed as detailed for the lipoxygenase enzyme full scan mode experiment.

Monitoring the Oxidation of LA, AA, *a*LA, and *a*AA to Completion. s15LOX1, LA, AA, *a*LA, and *a*AA were diluted to 2× final concentration in 100 mM borate pH 9 at 25 °C. One mL fatty acid was added to a 1 cm cuvette in a Beckman-Coulter DU-800 spectrophotometer and blanked. One mL enzyme was added, and the reaction was monitored at 235 nm sampling every 1.5 s, until the Δabsorbance reached 0. The data was fit to a one-phase exponential association in GraphPad Prism to get R^2 values and maximum absorbances.

NMR of *a*AA Metabolites. mCOX2 was incubated 5 min in 100 mM Tris, 500 μM phenol, and 2× [mCOX2] hematin pH 8 at 37 °C. *a*AA was added, and the reaction was allowed to proceed for 15 h at 37 °C. The reaction was extracted with two volumes ethyl acetate, and the organic layer was removed and evaporated under inert gas. The residue was dissolved in ethanol and separated by reverse-phase HPLC on a SUPELCOSIL C_{18} (150 mm × 3.0 mm, 5 μm) column, eluted with a linear gradient with A and B buffers consisting of 0.1% acetic acid in water and 0.1% acetic acid in acetonitrile. The gradient was held at 10% B for 10 min, then ramped to 100% B over the next 20 min, then held at 100% B for 5 min, all at the flow rate of 1.0 mL/min. The elution profile was monitored by absorbance at 235 nm. Peaks were collected, dried under inert gas, and dissolved in $CDCl_3$ for NMR analysis. ^1H and $^1H-^1H$ COSY spectra were recorded on Bruker AV-II 600 MHz spectrometer equipped with a cryoprobe. Chemical shifts are reported in parts per million relative to the signal of residual nondeuterated solvent.

LC/MS/MS-Based Kinetics for mCOX2. Metabolites of mCOX2 do not have an absorbance that can be used to perform kinetic measurements. Therefore, LC/MS/MS was used to measure kinetic parameters based on specific metabolites. mCOX2 was diluted to 25 nM in 100 mM Tris, 500 μM phenol, 50 nM hematin pH 8, and incubated at 37 °C. AA and *a*AA were added from 100× stocks in DMSO, and incubated at 37 °C. The length of incubation was optimized to give less than 20% substrate turnover. The reactions were quenched and fatty acid metabolites extracted with ethyl acetate containing 0.5% acetic acid, PGE_2-d_4, and 13-HODE-d_4. Metabolites were separated by reverse-phase gradient HPLC on a C_{18} (50 mm × 2.1 mm, 3 μm) column using 0.1% formic acid in water and 0.1% formic acid in acetonitrile as the A and B mobile phases, respectively. Metabolites were separated by holding 25% B for 0.5 min, then ramping to 99% B over 2.5 min, holding at 99% B for 3 min, then equilibrating to 25% B for 3 min. Metabolites were analyzed in negative ion mode by SRM, monitoring the transitions for *a*11-HETE (315.2 > 167.2), *a*PG (347.2 > 267.2), PG (351.2 > 271.2), 13-HODE-d_4 (299.2 > 198.2), PGE_2-d_4 (355.2 > 275.2) on an ABI/Sciex 3200 QTrap interfaced to a Shimadzu LC system. No deuterated standard exists for 11-HETE. The signal intensity ratio between *a*11-HETE and 13-HODE-d_4 was observed to be similar in both full scan MS and SRM modes, indicating that 13-HODE-d_4 can be used to quantify *a*11-HETE. The amount of each product formed was converted into a concentration, and then into initial reaction rates (V_o) using the incubation time. Kinetic parameters were determined in GraphPad Prism using Michaelis−Menten fitting.

RAW264.7 Macrophage Enrichment, Activation, and Measurement of *a*AA Metabolites. RAW264.7 macrophages (ATCC, Manassas, VA) were plated at 10% confluence in DMEM+Glutamax (Life Technologies, Grand Island, NY) supplemented with 10% fetal bovine serum (Atlas Biologicals, Fort Collins, CO). Fatty acid free BSA/*a*AA (6:1) was prepared as previously described.[29] After 24 h, media was replaced with serum free DMEM+Glutamax containing *a*AA/BSA added to 15 μM final concentration of *a*AA. After 24 h, the

dx.doi.org/10.1021/ja506038v | J. Am. Chem. Soc. 2014, 136, 11529−11539

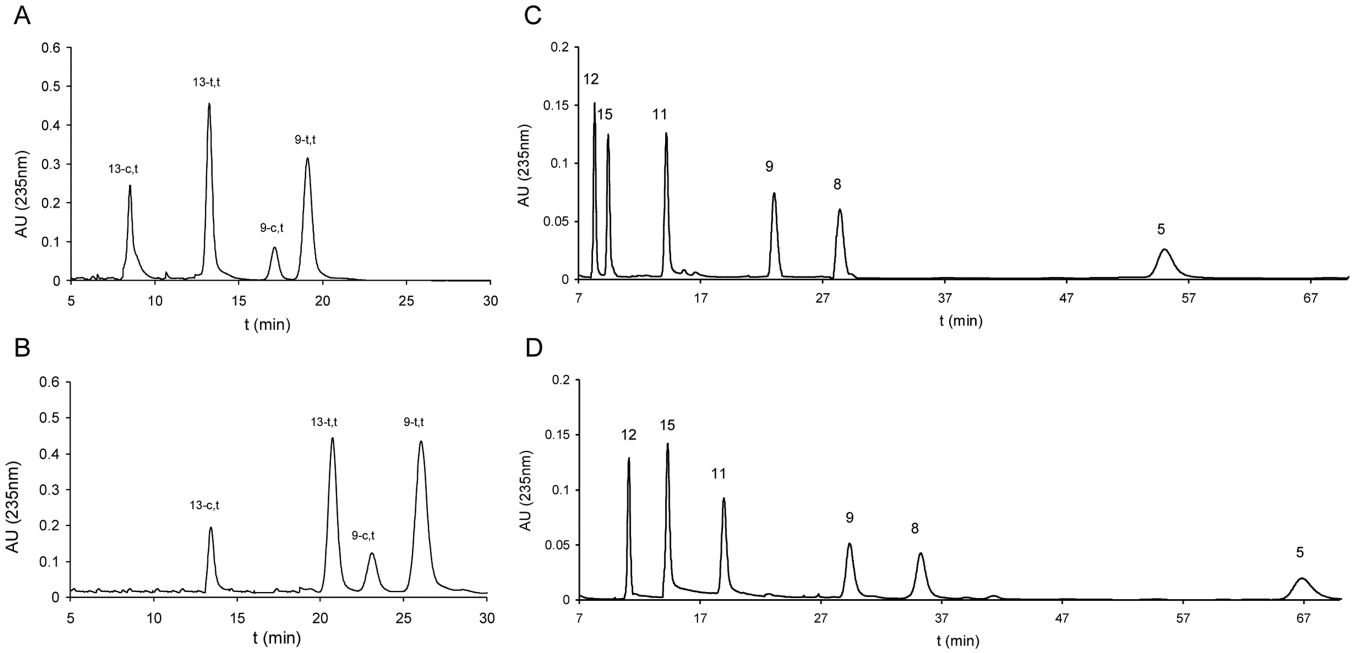

Figure 1. Autoxidation products of of LA (A), *a*LA (B), AA (C), *a*AA (D). LA/*a*LA peaks are labeled with the hydroxyl position on either the 9 or 13 carbon, and the double bond configuration which resulted in either *cis/trans* (c,t) or *trans/trans* (t,t). AA/*a*AA peaks are labeled with the position of the oxygen on either the 5, 8, 9, 11, 12, or 15 carbon. Both fatty acid pairs oxidize to similar product profiles with similar elution orders.

cells were washed with one volume DMEM+Glutamax to remove any unincorporated *a*AA, and treated with DMEM+Glutamax ±100 ng/mL Kdo_2-lipid A (KLA) (Avanti Polar Lipids, Alabaster, AL), prepared as previously described.[30] After 24 h, cells were scraped into media and extracted with two volumes ethyl acetate containing 0.5% acetic acid, PGE_2-d_4, and 13-HODE-d_4. The organic layer was dried under an inert gas stream and dissolved in methanol for LC/MS/MS analysis. Metabolites were separated by reverse-phase gradient HPLC on a C_{18} (50 mm × 2.1 mm, 3 μm) column using 0.1% formic acid in water and 0.1% formic acid in acetonitrile as the A and B mobile phases, respectively. Metabolites were separated by holding 25% B for 0.5 min, then ramping to 99% B over 2.5 min, holding at 99% B for 3 min, then equilibrating to 25% B for 3 min. Metabolites were analyzed in negative ion mode by SRM, monitoring the transitions for *a*11-HETE (315.2 > 167.2), *a*11-8,9-HEET (331.2 > 165.2), *a*PG (347.2 > 267.2), PG (351.2 > 271.2), 13-HODE-d_4 (299.2 > 198.2), and PGE_2-d_4 (355.2 > 275.2) on an ABI/Sciex 3200 QTrap interfaced to a Shimadzu controller, autosampler, and HPLC pumps.

RESULTS

LA and *a*LA were oxidized under conditions that would allow us to compare autoxidation rates and products. As shown in Figure 1, four ω-alkynyl conjugated diene hydroperoxides (alkynyl hydroperoxyoctadecadienoic acids, *a*HpODEs) were produced as primary products from *a*LA autoxidation, a result directly analogous to the chemistry observed with LA.[11] Reduction of the hydroperoxides to the corresponding alcohols, *a*HODEs, was carried out immediately after peroxidation since the HODEs are more stable and better suited for HPLC analysis than HpODEs. HPLC-UV analysis revealed that parallel oxidation of equimolar amounts of *a*LA and LA generated equivalent amounts of *a*HODEs and HODEs, with elution orders identical to those of the natural compounds.[11] The isolated products were then analyzed by ESI-MS and NMR to confirm hydroxyl position and conjugated diene geometry (Supporting Information [SI] Figure 1). Utilizing chiral chromatography, it was determined that the autoxidation of *a*LA produces a mixture of *R*- and *S*-HODE enantiomers, similar to that of LA (SI Figure 2).

Contrary to the simplicity of products generated from LA autoxidation, peroxidation of AA yielded a much more complex mixture of products. In addition to acyclic hydroxy and hydroperoxy products (HETEs and HpETEs) analogous to HODEs and HpODEs, a mixture of diastereomeric isoprostanes (IsoPs) was produced from AA peroxidation.[31−34] Oxidation of *a*AA under conditions that gave HpETEs as major products was promoted by NMBHA.[27] As shown in Figure 1, characterization of peroxidation products was performed on the *a*HETEs after reduction of the corresponding hydroperoxides. The HPLC−UV elution profile for *a*HETEs was similar to the profile obtained for their natural analogues. MS analyses established the position of oxygen substitution on the carbon chain (SI Table 1), and NMR analysis provided information about stereoisomeric geometry (SI Figure 1). The major HETE stereoisomers have *Z*,*E*-conjugated diene geometry, analogous to the structure of AA-derived HETEs. These experiments show that the elution order of *a*HETEs is identical to the elution order observed for HETEs. Additionally, oxidation of equimolar mixtures of AA and *a*AA generated nearly equimolar mixtures of HETE and *a*HETE.

HETEs are not the only autoxidation products formed from AA, so *a*AA was exposed to the radical initiator MeOAMVN in the absence of NMBHA under conditions of oxidation and workup that were expected to yield significant quantities of the *a*$F_{2\alpha}$-IsoPs. LC/MS/MS analysis of the major (*a*)$F_{2\alpha}$-IsoPs formed in this sequence are shown in SI Figure 3. Chromatograms of only the 5- and 15-series (*a*)$F_{2\alpha}$-IsoPs are presented because these compounds are formed in a large excess compared to the 8- and 12-regioisomers. The preference for formation of the 5- and 15-regioisomers and the elution profiles observed for both the natural and ω-alkynyl analogues are consistent with a previous report.[35]

dx.doi.org/10.1021/ja506038v | J. Am. Chem. Soc. 2014, 136, 11529−11539

Table 1. Kinetic Values Comparing *a*AA and AA for the Enzymes Ovine Cyclooxygenase 1 (oCOX1), Human Cyclooxygenase 2 (hCOX2), Human Platelet-Type 12 Lipoxygenase (plt12LOX), Porcine Leukocyte-Type 12 Lipoxgygenase (lk12LOX), Rabbit Reticulocyte 15 Lipoxygenase 1 (r15LOX1), and Soybean 15 Lipoxygenase 1 (s15LOX1)[a]

enzyme	substrate	product	K_m (μM)	V_{max} (μMs^{1-})	k_{cat} (s^{-1})	k_{cat}/K_m (μM^{-1} s^{-1})	V_{max}/K_m (s^{-1})
oCOX1	aAA	O_2 cons.	6.2 ± 0.8	n/a	57 ± 6	9 ± 6	n/a
	AA		(3.4 ± 0.6)		(51 ± 3)	(15 ± 3)	
hCOX2	aAA	O_2 cons.	4.5 ± 0.7	n/a	11 ± 1	2 ± 1	n/a
	AA		(6.1 ± 0.6)		(14.7 ± 0.5)	(2.4)	
plt12LOX	aAA	Abs 235 nm	7.0 ± 0.3	4.53 ± 0.08	n/a	n/a	0.6 ± 0.3
	AA		(9.5 ± 0.7)	(13.3 ± 0.3)			(1.4 ± 0.7)
lk12LOX	aAA	Abs 235 nm	4 ± 1	1.37 ± 0.09	n/a	n/a	0.3 ± 1
	AA		(7.8 ± 1.3)	(13.1 ± 0.7)			(2 ± 1)
r15LOX1	aAA	Abs 235 nm	7 ± 2	0.61 ± 0.05	n/a	n/a	0.09 ± 2
	AA		(20 ± 3)	(8.6 ± 0.4)			(0.4 ± 3)
s15LOX1	aAA	Abs 235 nm	3.1 ± 0.9	0.025 ± 0.002	2.5 ± 0.2	0.8 ± 0.2	n/a
	AA		6 ± 1	0.12 ± 0.01	24 ± 2	4.3 ± 0.2	

[a]All COX enzymes were assayed using oxygen electrode. LOX enzymes were assayed using absorbance at 235 nm. AA kinetic values taken from the literature are in parentheses.[1] V_{max}/K_m values are reported for crude enzyme preparations, while k_{cat}/K_m values are reported for purified enzymes.

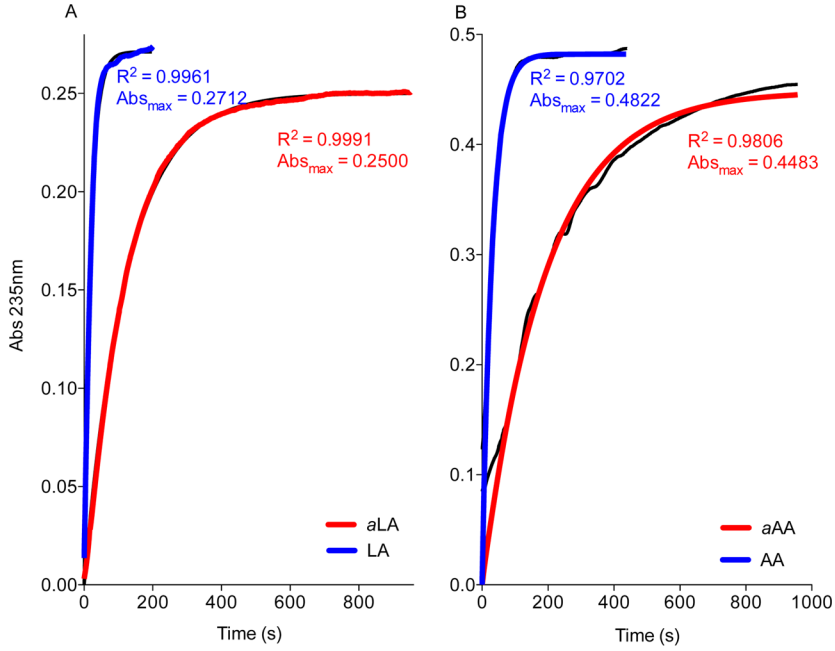

Figure 2. LA, *a*LA, AA, and *a*AA were all incubated with s15LOX1 and observed at 235 nm until ΔAbs = 0. Despite having different kinetic parameters, fatty acid pairs *a*LA/LA (A) and *a*AA/AA (B), are eventually oxidized completely.

Using alkynyl fatty acids to further probe the biochemistry of cellular systems requires detailed knowledge of the chemistry of enzymatic oxidation. Kinetic parameters were determined for the transformations of *a*AA in the presence of several LOX and COX enzymes by measuring alkene formation or O_2 consumption, respectively. Data presented in Table 1 demonstrate small differences in k_{cat}/K_M for the alkynyl and natural fatty acids, suggesting that *a*AA is an efficient substrate for both COX-1 and COX-2. The catalytic efficiency of human platelet-type 12-LOX in the presence of *a*AA was also found to be similar to the efficiency observed for AA as a substrate. On the other hand, porcine leukocyte-type 12-LOX, rabbit reticulocyte 15-LOX1, and s15-LOX1 did not oxidize *a*AA as efficiently as AA, illustrated by the relatively large differences in V_{max}/K_m and k_{cat}/K_m values between these substrates. Despite these differences in kinetic parameters, *a*AA is completely converted by a15LOX1 when reacted for long enough times (Figure 2).

The kinetic parameters for the transformations of *a*LA and LA by s15LOX1 were also measured, and k_{cat}/K_m values were determined to be 0.51 ± 0.07 μM^{-1} s^{-1} and 5.2 ± 0.6 μM^{-1} s^{-1}, respectively. These values are similar to those observed for *a*AA and AA (Table 1), and like *a*AA, *a*LA is also eventually completely reacted (Figure 2). *a*LA and LA give a similar product profile of primarily (*a*)9-HODE or (*a*)13-HODE for the enzymatic transformation by 5-LOX or s15-LOX1 respectively (SI Figures 4 and 5). *a*13-HODE produced from s15LOX1 was assessed for optical purity, and determined to be entirely the *S* isomer, as anticipated from the stereochemistry of LA oxidation (SI Figure 3). Ovine COX1 generated a product profile similar to that of mCOX2 when reacted with LA, and neither enzyme oxygenated *a*LA (SI Figure 5).

dx.doi.org/10.1021/ja506038v | J. Am. Chem. Soc. 2014, 136, 11529−11539

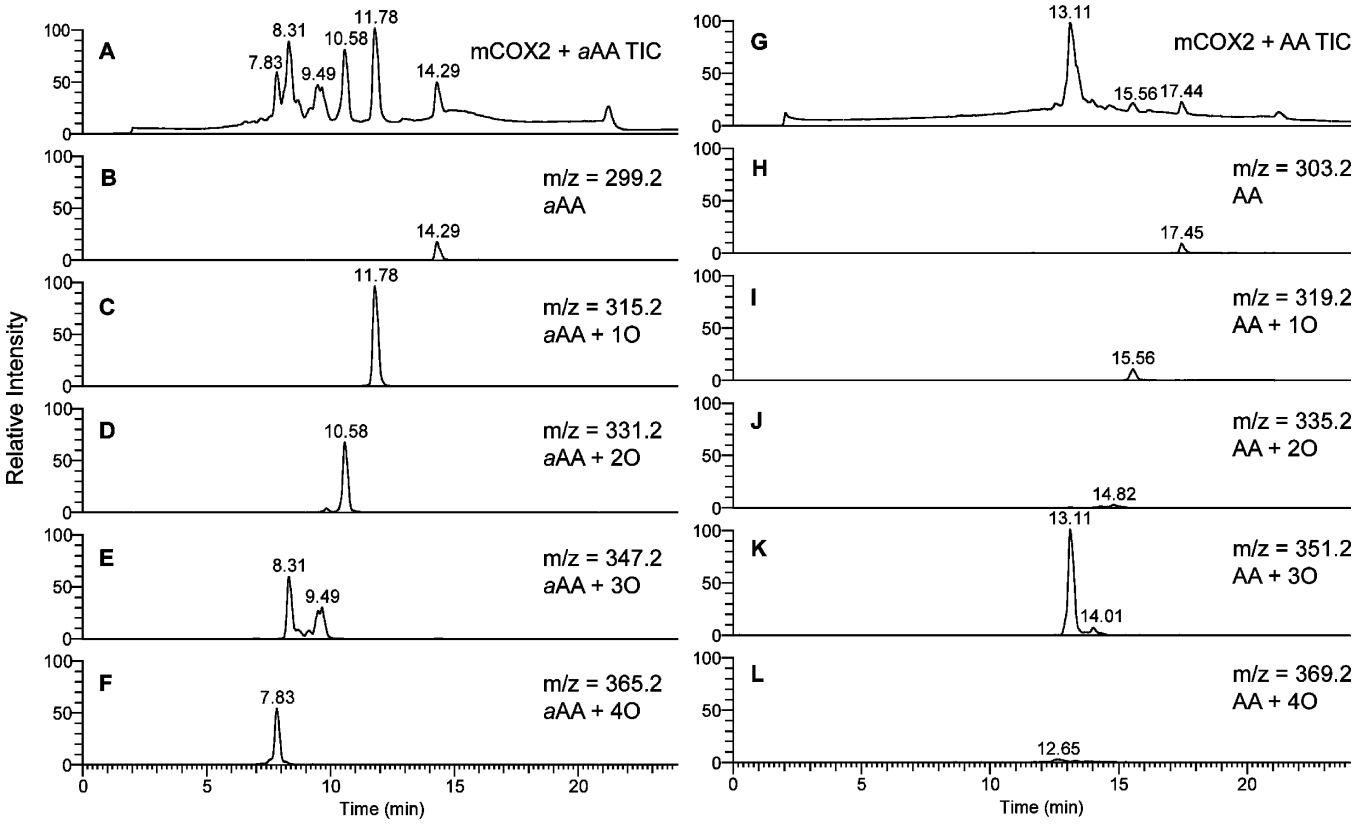

Figure 3. XIC analysis of the metabolite profiles of *a*AA (A) and AA (G) catalyzed by mCOX2 show very different products. The metabolism of *a*AA by mCOX2 shows some *a*AA remaining (B) and four products corresponding to the addition of one (C), two (D), three (E), and four (F) atoms of oxygen. The profiles in B–F are all to the same scale. The metabolism of AA by mCOX2 shows a single major product showing the addition of three atoms of oxygen and having the same m/z as PGE_2/PGD_2 (K). In addition to the major metabolite and remaining AA (H), metabolism of AA by mCOX2 shows three other products corresponding to the addition of one (I), two (J), and four (L) oxygens. These AA products correspond to the nonalkynylated versions of the products seen when *a*AA is metabolized by mCOX2. The profiles in H–L are to the same scale.

We compared the kinetics of mCOX2 oxidation of *a*AA determined by O_2 uptake (Table 1) to values determined by LC/MS/MS and noticed that the product profile from *a*AA was different from that of AA. As demonstrated in Figure 3, four *a*AA-derived oxygenation products were identified by MS, which correspond to the addition of one (m/z = 315.2), two (m/z = 331.2), three (m/z = 347.2), and four atoms of oxygen (m/z = 365.2). The product at m/z = 315.2 corresponds to *a*11-HETE, and the product at m/z = 347.2 corresponds to *a*PGE_2/D_2. One possibility for the identity of the product at m/z = 331.2 is *a*HpETE; however, attempted reduction of the hydroperoxide with either TCEP or PPh_3 did not alter the peak elution time (data not shown), indicating a chemically distinct species from the hydroperoxide. Although the metabolite profile of AA by mCOX2 resulted in peaks with m/z values corresponding to the addition of one, two, three, and four atoms of oxygen, similar to what was seen with *a*AA, the intensity of the peaks displayed major differences. AA oxygenation by mCOX2 results in a major peak at m/z = 351.2, corresponding to PGE_2/D_2, and a minor peak at m/z = 319.2, corresponding to a single oxygen atom incorporation. The remaining oxygen addition peaks were very minor by comparison, but have similar retention time and molecular weight shifts relative to PG as was seen with *a*AA. Ovine COX1 generated a product profile similar to that of mCOX2 for *a*AA and AA (data not shown).

To identify the metabolites depicted in Figure 3, product peaks at m/z = 315.2 and 331.2 were isolated and analyzed via 1D and 2D NMR. The compound present at m/z = 365.2 was not stable through the isolation process and thus was not analyzed. Figure 4 shows the structure and $^1H-^1H$ COSY for the peak at m/z = 315.2. It was determined that the identity of this peak is (5*Z*, 8*Z*, 12*E*,14*Z*)-11-hydroxyeicosa-5,8,12,14-tetraen-19-ynoic acid (alkynyl 11-hydroxyeicosatetraenoic acid, *a*11-HETE). SI Table 2 shows the chemical shifts relative to $CDCl_3$ and coupling constants as determined from the ^1H NMR (SI Figure 6). The coupling constants for the alkene between C12 and C13, $J_{12,13}$ = 15.2 and 15.1 Hz respectively, identify the bond as *trans*. Figure 5 shows the structure and $^1H-^1H$ COSY for the peak at m/z = 331.2. It was determined that the identity of this peak is (*Z*)-7-(3-((3*E*, 5*Z*)-2-Hydroxyundeca-3,5-dien-10-yn-1-yl)oxiran-2-yl)hept-5-enoic acid (alkynyl 11-hydroxy-8,9-epoxy-eicosatrienoic acid, *a*11-8,9-HEET). SI Table 3 shows the chemical shifts relative to $CDCl_3$ and coupling constants as determined from the ^1H NMR (SI Figure 7). The coupling constants $J_{12,13}$ = 15.2 and 15.1 Hz, assign the alkene between C12 and C13 as *trans*. The coupling constants for the epoxide were measured as $J_{8,9}$ = 4.2 and 4.3 Hz, identifying the epoxide as *cis*.

Due to the distinct product profile of *a*AA metabolism, the kinetic parameters for *a*AA were reevaluated by LC/MS/MS. AA kinetic parameters were determined using the product PGE_2, whereas the kinetic parameters for *a*AA were determined

dx.doi.org/10.1021/ja506038v | J. Am. Chem. Soc. 2014, 136, 11529–11539

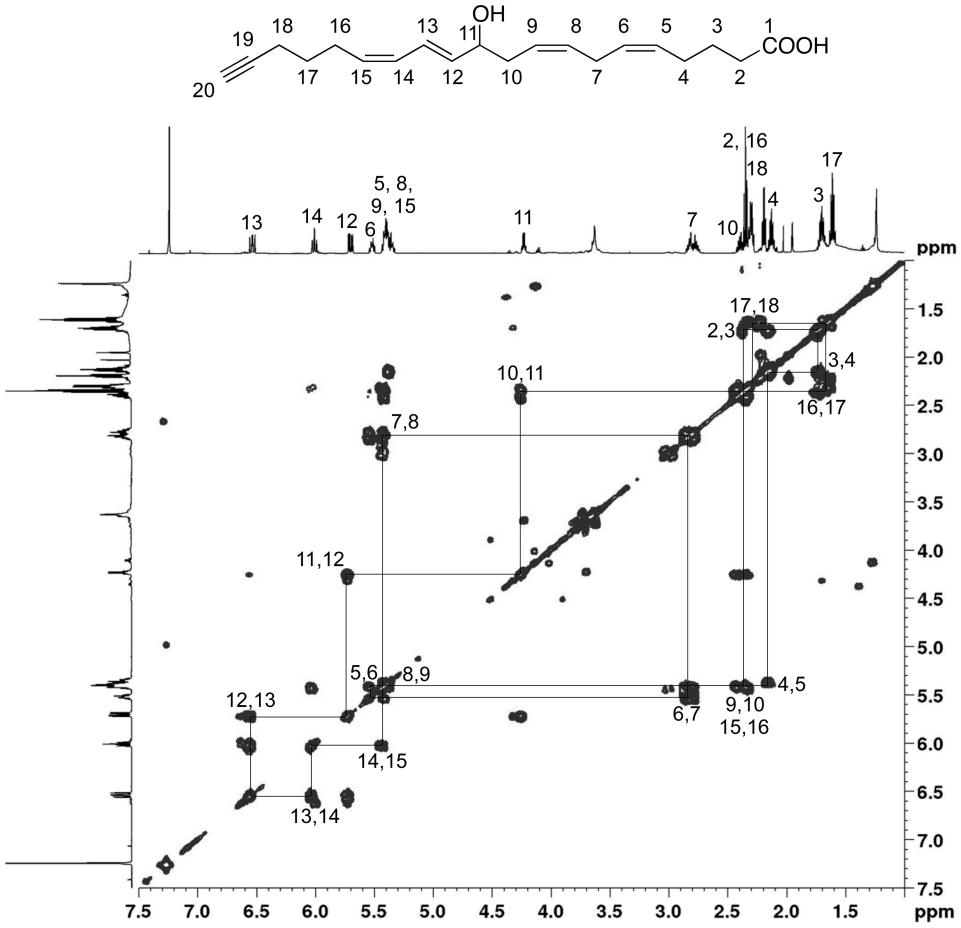

Figure 4. $^{1}H-^{1}H$ COSY spectrum of the collected LC/MS peak with m/z = 315.2 with peaks assigned, which was identified to be that of *a*11-HETE.

using *a*PGE$_2$ and *a*11-HETE. Michaelis–Menten plots for these three kinetic experiments are found in Figure 6. The catalytic efficiency for the formation of PGE$_2$ by mCOX2, 1.6 ± 0.2 μM^{-1} s^{-1}, was similar to the oxygen uptake value for hCOX2 seen in Table 1. The small difference between the two can be explained by the formation of the nonenzymatic PG degradation product, 12-hydroxyheptadecatrienoic acid (HHT), which accounts for approximately 20% of the total PG signal (data not shown). The catalytic efficiencies for *a*AA products were very different, however, at 0.019 ± 0.005 μM^{-1} s^{-1} for *a*PG formation and 0.4 ± 0.1 μM^{-1} s^{-1} for *a*11-HETE formation. When these values are compared to the hCOX2 oxygen uptake during *a*AA metabolism value, 2 ± 1 μM^{-1} s^{-1}, it can be seen that most of the oxygen consumption is due to the formation of *a*11-HETE.

To evaluate the potential of *a*AA as a tool in cellular settings, its incorporation, release, and metabolism was tested in RAW264.7 macrophages. BSA/*a*AA complexes were formed as previously described and then were added to serum-free cell culture medium for 24 h.[29] Cells were then washed with medium to remove any unincorporated *a*AA and activated with 100 ng/mL KLA for 24 h. Fatty acid metabolites were extracted from the combined media and cells. Figure 7 shows the quantification of *a*11-HETE, *a*11-8,9-HEET, *a*PG, and PG in cells enriched with *a*AA and activated with KLA. The alkynylated products were only seen at high levels in the *a*AA-enriched and KLA-activated cells, which corresponds to the conditions where levels of fatty acid release and COX2 expression are highest. Further correlating to the kinetic and *in vitro* experiments, *a*11-HETE was more abundant than *a*PG and *a*11-8,9-HEET in cells. The ratio of *a*11-HETE to *a*PG and *a*11-8,9-HEET is increased from the purified protein analyses indicating that cellular and purified enzyme metabolite profiles may have slight differences.

DISCUSSION

Understanding both the enzymatic and nonenzymatic metabolism of alkynyl fatty acids is important because lipid oxygenation products and lipid electrophile formation has been reported to result from both enzymatic and nonenzymatic mechanisms.[36−38] Our data indicate that *a*LA and LA are kinetically equivalent substrates for free radical chain oxidation; (*a*)HODEs are formed as two positional isomers with oxidation at the 9 and 13 carbons. Additionally, the conjugated dienes are in two different conformations, the *ZE* kinetic product, and the *EE* thermodynamic product. Analyzing the *ZE/EE* product ratios can be used as a "peroxyl radical clock" to measure peroxidation propagation rate constants,[39] further confirming that these two substrates are equivalently oxidized.

Similarly, *a*AA and AA are also equivalent substrates for autoxidation. The mechanism of HpETE and IsoP formation has been studied in great detail and it has been established that six major *Z,E*-HpETE products form with hydroperoxide substitution at carbons 5, 8, 9, 11, 12, and 15 of the 20 carbon eicosanoate chain.[40] The IsoPs are formed as a mixture of stereoisomers, the four sets of regioisomers identified by the position of the allylic alcohol in the chain, 5, 8, 12, and 15.[41] Each regioisomeric set of IsoPs contains eight diasteromers.

dx.doi.org/10.1021/ja506038v | J. Am. Chem. Soc. 2014, 136, 11529−11539

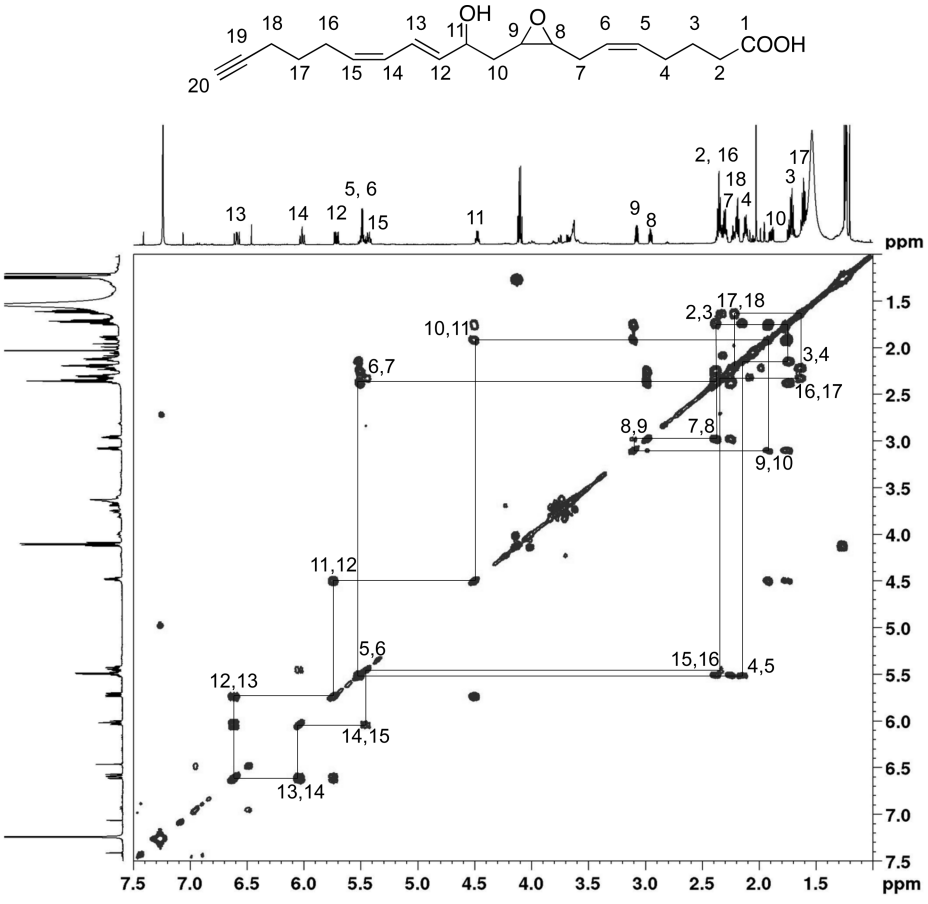

Figure 5. $^{1}H-^{1}H$ COSY spectrum of the collected LC/MS peak with m/z = 331.2 with peaks assigned, which was identified to be that of *a*11-8,9-HEET.

Quantification of the IsoP isomeric mixture has been used in recent years as a measure of oxidative stress *in vivo*.[8,42,43] Both *a*AA and AA form the respective HpETEs and IsoPs at similar levels. This is an important finding for setting up future lipid oxidation studies since many disease states, including models for cardiovascular disease and neurodegenerative diseases, are characterized by a high level of oxidative stress.[7]

The kinetic values measured here indicate that with some notable exceptions, *a*AA is a reasonable enzymatic substrate for both COX and LOX classes of enzymes. Enzymatically, both alkynyl PUFAs are metabolized by various LOX enzymes to product profiles similar to those of the native PUFAs. Despite the observed differences in catalytic efficiency, *a*AA, AA, *a*LA, and LA are completely oxygenated by s15LOX1 when allowed to react to completion (Figure 2). We hypothesize that the reduced efficiency observed is the result of the alkyne altering the conformation of the lipid within the LOX active site. Model systems designed to study cellular processes all have limitations, and the reduced enzymatic efficiency seen here may restrict the use of this model to understand short-term enzymatic lipid metabolism. However, in many biological settings, this reduced enzymatic efficiency remains negligible in understanding and tracking lipid metabolism because many studies will be looking at changes over long time periods.

These data demonstrate the potential usefulness of *a*PUFAs for the study of lipids in a biological setting; however, one major finding is the differential metabolism of AA and *a*AA by mCOX2 and oCOX1. All of the products in our proposed mechanism (Scheme 1) result from the same first two steps, 13-(*S*)-hydrogen abstraction and oxygen addition to C11 forming the alkynyl 11-hydroperoxyl radical. The remaining reactions proceed through two critical junctions, endoperoxide formation and prostaglandin ring closure. The *a*11-hydroperoxyl radical can be reduced by H atom transfer to form *a*11-HETE (Scheme 1A), which was identified as one of the major products by LC/MS/MS and 2D-NMR (Figure 4). When endoperoxide formation is followed by prostaglandin ring closure, and a final oxygenation at C15, *a*PGG_2, the precursor to all prostaglandins is formed (Scheme 1B). However, when endoperoxide formation is not followed by prostaglandin ring closure, endoperoxide homolytic cleavage results in 8,9-epoxide and 11-alkoxyl radical formation. The alkoxyl radical can then be terminated to give *a*11-8,9-HEET (Scheme 1C), which was identified by 2D-NMR (Figure 5). The epoxide was identified as *cis* due to the coupling constants for H8 and H9, which were measured at 4.2 and 4.3 Hz, respectively. This is an interesting observation indicating that the epoxide is formed in the enzyme active site, before the bond between C7 and C8 can rotate. Nonenzymatic epoxidation from endoperoxide scission would be expected to give a 3:1 *trans:cis* geometry due to the free rotation of the C7−C8 bond.[44] 11-8,9-HEET was first identified when 8,9 epoxy-eicosatrienoic acid was incubated with cyclooxygenase enzymes. The cyclooxygenase enzymes were only able to add oxygen to C11 because the epoxide prevented endoperoxide formation.[45,46] The major mCOX2 products of *a*AA oxygenation we have identified are structurally similar to previously reported COX2 variant AA metabolites.[47] Schneider et al. demonstrated that mutations at Gly526 and

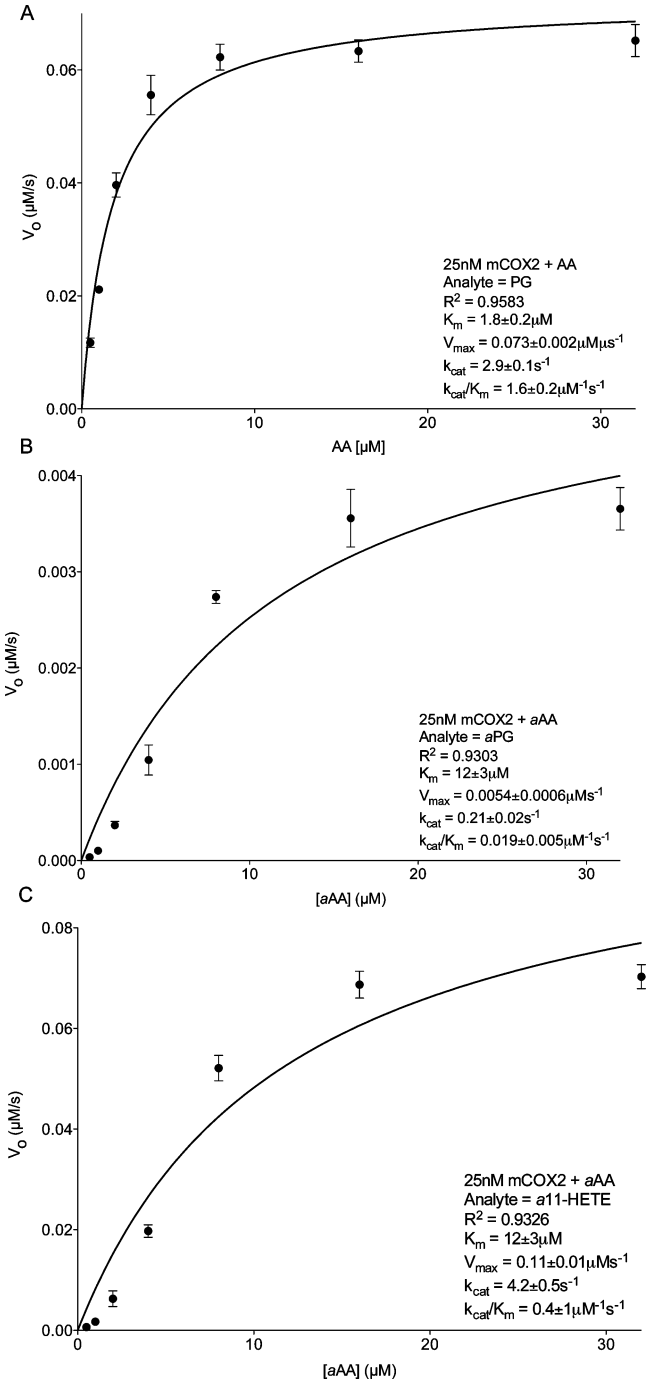

Figure 6. Michaelis–Menten plots and relevant kinetic parameters for mCOX2 metabolism of AA and *a*AA measuring the formation of prostaglandins (A), alkynyl prostaglandins (B), and alkynyl 11-HETE (C).

Leu384 to larger amino acids restrict endoperoxide formation and prostaglandin ring closure, resulting in the generation of multiple products including 11-HpETE and PGs. Their proposed mechanism proceeds through several intermediates that, when terminated, will give the AA-derived products similar to those we have identified.

While we have been unable to solve a crystal structure of *a*AA in a productive conformation in the mCOX2 active site, we can look at other substrates to corroborate the idea that *a*AA may not be binding properly in the active site, resulting in

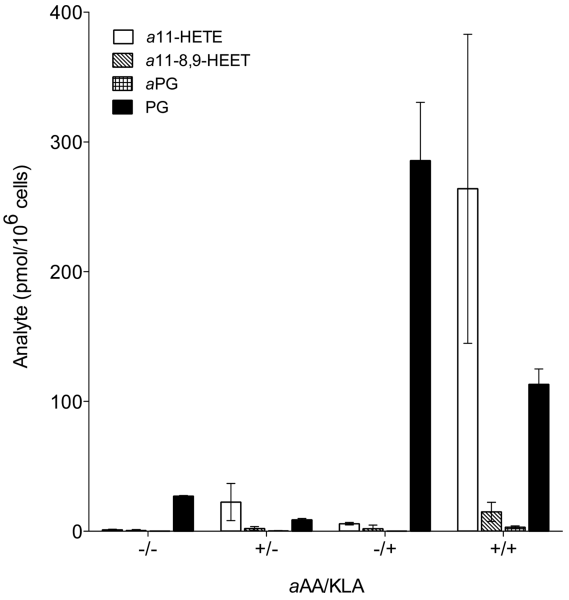

Figure 7. RAW264.7 macrophages were enriched ±*a*AA, then activated with ±100 ng/mL KLA for 24 h. Metabolite levels were measured by LC/MS/MS-SRM for the media and cells combined.

an altered product profile. One substrate that can be investigated is the endocannabinoid 2-arachidonylglycerol (2-AG). The crystal structure of its isomer, 1-AG, has been solved for mCOX2, and it was revealed that it sits in the active site in two different conformations. The structural difference in these confirmations is a slight change in the position of the ω-tail in the active site. Oxygenation may occur in both conformations because abstractable hydrogens on C13 are in line with the catalytic Tyr385, but different distances in each conformation.[48] 2-AG has two major products, PG-glycerol and 11-HETE-glycerol,[49] which further corroborates that there are multiple modes of binding. These data are potentially relevant to *a*AA binding in the mCOX2 active site, because they indicate that small changes in the binding of the ω-tail has an impact on the oxygenation and cyclization events at the center of the fatty acid. Therefore, we hypothesize that the alkynyl tail changes the way *a*AA sits in the COX2 active site, resulting in similar O_2 consumption despite its altered product profile, as defined in these studies.

On the basis of all of the *in vitro* oxidation, we investigated the viability of alkynyl probes for the analysis of lipid metabolite detection and tracking in a biological setting. RAW264.7 macrophages are the prototypical cell line used to study lipid metabolism because their lipid chemistry has been extensively cataloged by the Lipid MAPS Consortium (www.lipidmaps.org). Therefore, we investigated if the *in vitro* mCOX2 metabolites of *a*AA could be measured in cultured cells and observed *a*11-HETE as the major *a*AA metabolite in cells, with *a*PG and *a*11-8,9-HEET also detected, but at a much lower level. This product ratio matches the kinetic efficiencies measured *in* vitro for *a*11-HETE and *a*PG formation. Many molecules have been reported to potentiate COX2 activity *in vitro*, including free fatty acids.[50] It is not unreasonable to think that many of these species are present in cells, and could potentiate the formation of *a*11-HETE as was seen in our data. 11-HETE has been reported in many animal and cell models as a COX2-derived metabolite.[51−54] Additionally, it has been reported that hydroxy fatty acid metabolites of COX2,

dx.doi.org/10.1021/ja506038v | J. Am. Chem. Soc. 2014, 136, 11529−11539

Scheme 1. Proposed Mechanism of mCOX2 Oxygenation of *a*AA[a]

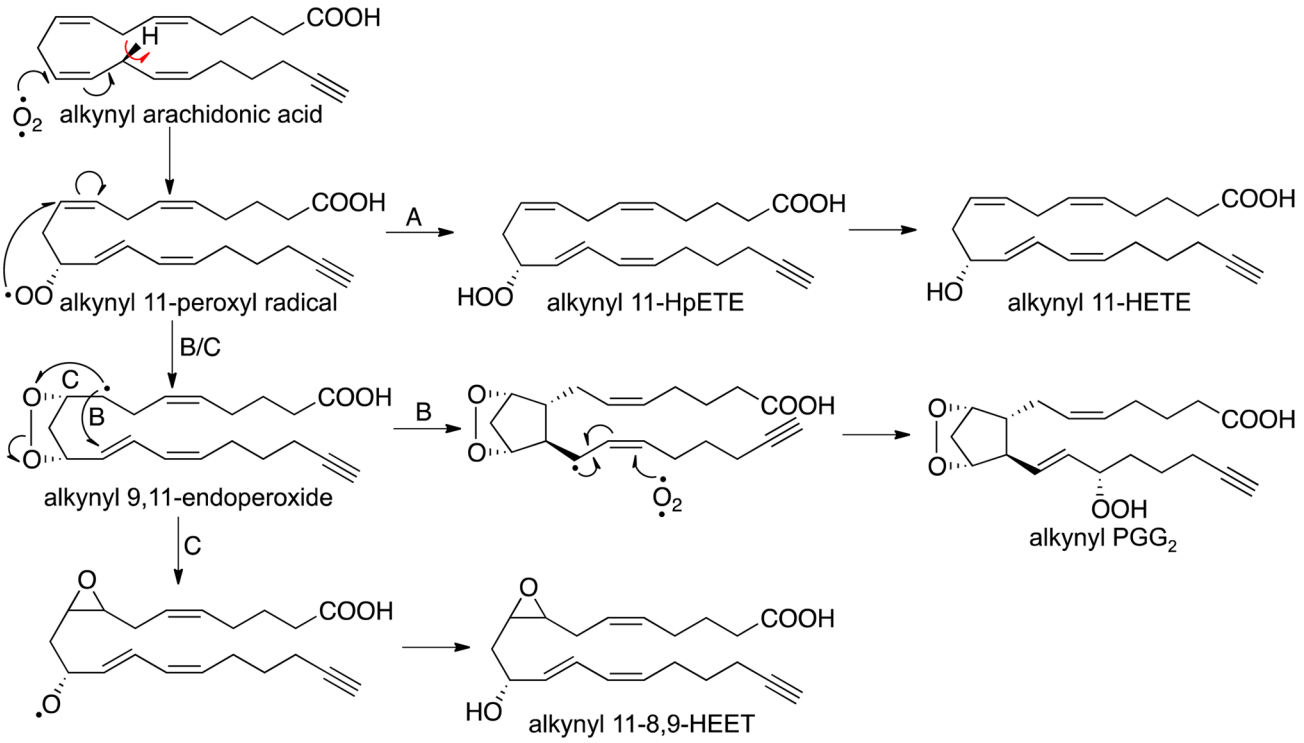

[a] All products result from the same first steps, abstraction of the 13-(*S*)-hydrogen and addition of molecular oxygen to the 11-carbon. Pathway A shows the formation of *a*11-HETE when the reaction is terminated before 9,11-endoperoxide is formation. After endoperoxide formation, closure of the 5-membered prostaglandin ring results in pathway B and the formation of *a*PGG_2, the precursor for all *a*PGs. However, if ring closure does not occur (pathway C), the endoperoxde can cleave, resulting in an epoxide and an 11-alkoxyl radical. The alkoxyl radical can be terminated to form *a*11-8,9-HEET.

including 11-HETE,[55,56] can be further oxidized by cellular dehydrogenases to oxo fatty acids.[36] These oxo fatty acids are electrophilic, reacting with nucleophilic amino acids of proteins potentially changing cellular functions. Prostaglandins are not readily converted to electrophilic species; thus, hydroxy fatty acids are the most viable method to study this chemistry in cells. 11-Oxoeicosatetraenoic acid, the oxidized product of 11-HETE, has been detected in cells, and shown to be antiproliferative.[55,56] This avenue of exploration is potentially viable using *a*AA as a part of a COX2-mediated metabolite study, in the appropriate context.

CONCLUSION

Collectively, these studies demonstrate that *a*PUFAs are metabolized similarly to native PUFAs and represent a viable tool for studying lipid distribution, metabolism, and reactions between lipid metabolites and cellular macromolecules in many physiological and pathophysiological models. While there are some caveats regarding the enzymatic metabolism of *a*AA, specifically the metabolism of these surrogates by the cyclooxygenase enzymes, the nonenzymatic metabolism is indistinguishable from that of the native lipid species. Therefore, *a*PUFAs can be used as analogues for PUFAs, especially in cellular disease models involving high amounts of oxidative stress resulting in high levels of lipid oxidation.

ASSOCIATED CONTENT

Supporting Information

This material is available free of charge via the Internet at http://pubs.acs.org.

AUTHOR INFORMATION

Corresponding Author

n.porter@vanderbilt.edu

Present Addresses

[⊥]Department of Chemistry, Imperial College of London, South Kensington Campus, Exhibition Road, London SW7 2AZ, UK. [#]Department of Molecular Toxicology, University of California Berkeley, Berkeley, CA 94720, United States.

Author Contributions

[‖]W.N.B. and R.S. contributed equally to this research.

Notes

The authors declare no competing financial interest.

ACKNOWLEDGMENTS

The authors would like to thank Don Stec at the Vanderbilt University Small Molecule NMR Center. We would also like to thank the Vanderbilt University Mass Spectrometry Resource Center. For editorial input, we would like to thank James Galligan. For funding sources we would like to thank the National Institutes of Health Grants R01 HD064727 (N.A.P.) and R37 CA087819 (L.J.M.), the National Science Foundation Grant CHE-1057500 (N.A.P.), and the American Heart Association Grant 13PRE17270009 (W.N.B.).

REFERENCES

(1) Prusakiewicz, J.; Turman, M.; Vila, A.; Ball, H.; Al-Mestarihi, A.; Marzo, V.; Marnett, L. *Arch. Biochem. Biophys.* **2007**, *464*, 260.
(2) Quehenberger, O.; Armando, A. M.; Brown, A. H.; Milne, S. B.; Myers, D. S.; Merrill, A. H.; Bandyopadhyay, S.; Jones, K. N.; Kelly, S.;

Shaner, R. L.; Sullards, C. M.; Wang, E.; Murphy, R. C.; Barkley, R. M.; Leiker, T. J.; Raetz, C. R.; Guan, Z.; Laird, G. M.; Six, D. A.; Russell, D. W.; McDonald, J. G.; Subramaniam, S.; Fahy, E.; Dennis, E. A. *J. Lipid Res.* **2010**, *51*, 3299.
(3) Andreou, A.; Feussner, I. *Phytochemistry* **2009**, *70*, 1504.
(4) Buczynski, M. W.; Dumlao, D. S.; Dennis, E. A. *J. Lipid Res.* **2009**, *50*, 1015.
(5) Coffa, G.; Schneider, C.; Brash, A. R. *Biochem. Biophys. Res. Commun.* **2005**, *338*, 87.
(6) Rouzer, C.; Marnett, L. *Chem. Rev.* **2003**, *103*, 2239.
(7) Nathan, C.; Ding, A. *Cell* **2010**, *140*, 871.
(8) Davis, T. A.; Gao, L.; Yin, H.; Morrow, J. D.; Porter, N. A. *J. Am. Chem. Soc.* **2006**, *128*, 14897.
(9) Porter, N. A. *Acc. Chem. Res.* **1986**, *19*, 262.
(10) Porter, N. A.; Weber, B. A.; Weenen, H.; Khan, J. A. *J. Am. Chem. Soc.* **1980**, *102*, 5597.
(11) Porter, N. A.; Wujek, D. G. *J. Am. Chem. Soc.* **1984**, *106*, 2626.
(12) Porter, N.; Caldwell, S.; Mills, K. *Lipids* **1995**, *30*, 277.
(13) Esterbauer, H. *Patholog.-Biolog.* **1996**, *44*, 25.
(14) Esterbauer, H.; Cheeseman, K. H. *Methods Enzymol* **1990**, *186*, 407.
(15) Esterbauer, H.; Zollner, H. *Free Radical Biol. Med.* **1989**, *7*, 197.
(16) Vila, A.; Tallman, K.; Jacobs, A.; Liebler, D.; Porter, N.; Marnett, L. *Chem. Res. Toxicol.* **2008**, *21*, 432.
(17) Milne, S.; Ivanova, P.; Forrester, J.; Alex Brown, H. *Methods* **2006**, *39*, 92.
(18) Berliner, J. A.; Zimman, A. *Chem. Res. Toxicol.* **2007**, *20*, 849.
(19) Brown, H. A.; Murphy, R. C. *Nat. Chem. Biol.* **2009**, *5*, 602.
(20) Rouzer, C.; Ivanova, P.; Byrne, M.; Milne, S.; Marnett, L.; Brown, H. *Biochemistry* **2006**, *45*, 14795.
(21) Myers, D. S.; Ivanova, P. T.; Milne, S. B.; Brown, H. A. *Biochim. Biophys. Acta* **2011**, *1811*, 748.
(22) Milne, S.; Tallman, K.; Serwa, R.; Rouzer, C.; Armstrong, M.; Marnett, L.; Lukehart, C.; Porter, N.; Brown, H. *Nat. Chem. Biol.* **2010**, *6*, 205.
(23) Tallman, K.; Armstrong, M.; Milne, S.; Marnett, L.; Brown, H.; Porter, N. *J. Lipid Res.* **2013**, *54*, 859.
(24) Kim, H.; Tallman, K.; Liebler, D.; Porter, N. *Mol. Cell. Proteomics* **2009**, *8*, 2080.
(25) Codreanu, S. G.; Ullery, J. C.; Zhu, J.; Tallman, K. A.; Beavers, W. N.; Porter, N. A.; Marnett, L. J.; Zhang, B.; Liebler, D. C. *Mol. Cell. Proteomics: MCP* **2014**, *13*, 849.
(26) Windsor, K.; Genaro-Mattos, T.; Kim, H.; Liu, W.; Tallman, K.; Miyamoto, S.; Korade, Z.; Porter, N. *J. Lipid Res.* **2013**, *54*, 2842.
(27) Punta, C.; Rector, C. L.; Porter, N. A. *Chem. Res. Toxicol.* **2005**, *18*, 349.
(28) Liu, W.; Yin, H.; Akazawa, Y. O.; Yoshida, Y.; Niki, E.; Porter, N. A. *Chem. Res. Toxicol.* **2010**, *23*, 986.
(29) Van Harken, D.; Dixon, C.; Heimberg, M. *J. Biol. Chem.* **1969**, *244*, 2278.
(30) Raetz, C.; Garrett, T.; Reynolds, C.; Shaw, W.; Moore, J.; Smith, D.; Ribeiro, A.; Murphy, R.; Ulevitch, R.; Fearns, C. *J. Lipid Res.* **2006**, *47*, 1097.
(31) Morrow, J. D. *Drug Metab. Rev.* **2000**, *32*, 377.
(32) Morrow, J. D.; Awad, J. A.; Boss, H. J.; Blair, I. A.; Roberts, L. J., 2nd *Proc. Natl. Acad. Sci. U.S.A.* **1992**, *89*, 10721.
(33) Morrow, J. D.; Minton, T. A.; Roberts, L. J., 2nd *Prostaglandins* **1992**, *44*, 155.
(34) Morrow, J. D.; Roberts, L. J., 2nd *Methods Enzymol.* **1999**, *300*, 3.
(35) Yin, H.; Porter, N. A. *Antioxid. Redox Signaling* **2005**, *7*, 170.
(36) Groeger, A. L.; Cipollina, C.; Cole, M. P.; Woodcock, S. R.; Bonacci, G.; Rudolph, T. K.; Rudolph, V.; Freeman, B. A.; Schopfer, F. J. *Nat. Chem. Biol.* **2010**, *6*, 433.
(37) Liu, W.; Porter, N.; Schneider, C.; Brash, A.; Yin, H. *Free Radical Biol. Med.* **2011**, *50*, 166.
(38) Schneider, C.; Porter, N.; Brash, A. *J. Biol. Chem.* **2008**, *283*, 15539.
(39) Roschek, B., Jr.; Tallman, K. A.; Rector, C. L.; Gillmore, J. G.; Pratt, D. A.; Punta, C.; Porter, N. A. *J. Org. Chem.* **2006**, *71*, 3527.
(40) Porter, N.; Logan, J.; Kontoyiannidou, V. *J. Org. Chem.* **1979**, *44*, 3177.
(41) Yin, H.; Gao, L.; Tai, H. H.; Murphey, L. J.; Porter, N. A.; Morrow, J. D. *J. Biol. Chem.* **2007**, *282*, 329.
(42) Yin, H.; Havrilla, C. M.; Gao, L.; Morrow, J. D.; Porter, N. A. *J. Biol. Chem.* **2003**, *278*, 16720.
(43) Yin, H.; Havrilla, C. M.; Morrow, J. D.; Porter, N. A. *J. Am. Chem. Soc.* **2002**, *124*, 7745.
(44) Porter, N.; Nixon, J. *J. Am. Chem. Soc.* **1978**, *100*, 7116.
(45) Zhang, J. Y.; Prakash, C.; Yamashita, K.; Blair, I. A. *Biochem. Biophys. Res. Commun.* **1992**, *183*, 138.
(46) Homma, T.; Zhang, J. Y.; Shimizu, T.; Prakash, C.; Blair, I. A.; Harris, R. C. *Biochem. Biophys. Res. Commun.* **1993**, *191*, 282.
(47) Schneider, C.; Boeglin, W. E.; Brash, A. R. *J. Biol. Chem.* **2004**, *279*, 4404.
(48) Vecchio, A.; Malkowski, M. *J. Biol. Chem.* **2011**, 1.
(49) Kozak, K. R.; Rowlinson, S. W.; Marnett, L. J. *J. Biol. Chem.* **2000**, *275*, 33744.
(50) Dong, L.; Vecchio, A. J.; Sharma, N. P.; Jurban, B. J.; Malkowski, M. G.; Smith, W. L. *J. Biol. Chem.* **2011**, *286*, 19035.
(51) Bailey, J. M.; Bryant, R. W.; Whiting, J.; Salata, K. *J. Lipid Res.* **1983**, *24*, 1419.
(52) Buczynski, M.; Stephens, D.; Bowers-Gentry, R.; Grkovich, A.; Deems, R.; Dennis, E. *J. Biol. Chem.* **2007**, *282*, 22834.
(53) Dennis, E.; Deems, R.; Harkewicz, R.; Quehenberger, O.; Brown, H.; Milne, S.; Myers, D.; Glass, C.; Hardiman, G.; Reichart, D. *J. Biol. Chem.* **2010**, *285*, 39976.
(54) Norris, P.; Reichart, D.; Dumlao, D.; Glass, C.; Dennis, E. *J. Leukocyte Biol.* **2011**, *90*, 563.
(55) Liu, X.; Zhang, S.; Arora, J. S.; Snyder, N. W.; Shah, S. J.; Blair, I. A. *Chem. Res. Toxicol.* **2011**, *24*, 2227.
(56) Snyder, N. W.; Revello, S. D.; Liu, X.; Zhang, S.; Blair, I. A. *J. Lipid Res.* **2013**, *54*, 3070.